Author Draft of the accepted IEEE Trans on Components, Packaging and Manufacturing Technology 2019.

Investigation of Simultaneous Effects of Surface Roughness, Porosity and Magnetic Field of Rough Porous Micro-Fin under a Convective-Radiative Heat Transfer for Improved Microprocessors Cooling of Consumer Electronics

George A. Oguntala, *Member, IEEE*, Gbeminiyi M. Sobamowo, Eya N. Nnabuike and Raed A. Abd Alhameed, *Senior Member, IEEE*

Abstract — **The ever-increasing demand for high-processing electronic systems has unequivocally called for improved microprocessor performance. However, increasing microprocessor performance requires increasing power and on-chip power density, both of which are associated with increased heat dissipation. Electronic cooling using fins have been identified as a reliable cooling approach. However, an investigation into the thermal behaviour of fin would help in the design of miniaturized, effective heatsinks for reliable microprocessor cooling. The aim of this paper is to investigates the simultaneous effects of surface roughness, porosity and magnetic field on the performance of a porous micro-fin under a convective-radiative heat transfer mechanism. The developed thermal model considers variable thermal properties according to linear, exponential and power laws, and are solved using Chebychev spectral collocation method. Parametric studies are carried using the numerical solutions to establish the influences of porosity, surface roughness, and magnetic field on the micro-fin thermal behaviour. Following the results of the simulation, it is established that the thermal efficiency of the micro-fin is significantly affected by the porosity, magnetic field, geometric ratio, nonlinear thermal conductivity parameter, thermo-geometric parameter and the surface roughness of the micro-fin. However, the performance of the micro-fin decreases when it operates only in a convective environment. In addition, we establish that the fin efficiency ratio which is the ratio of the efficiency of the rough fin to the efficiency of the smooth fin is found to be greater than unity when the rough and smooth fins of equal geometrical, physical, thermal and material properties are subjected to the same operating condition. The investigation establishes that improved thermal management of electronic systems would be achieved using rough surface fins with porosity under the influences of the magnetic field.**

Index Terms — Electronic cooling, thermal management, heatsink, micro-fin, surface roughness, microprocessor cooling.

I. Introduction

The semiconductor industry has witnessed a revolutionary increase in the past few decades leading to the development of high-processing computers and electronic systems. This evolution has subsequently seen a rising demand for high-performance computers and electronic systems. One key component in the middle of this evolutionary development is the microprocessor. Following Moore's law [1], recent microprocessors are designed with doubled transistor density every two years to achieve increased performance and increased on-chip power density with each new technology generation [2]. In addition, recent computer and electronic systems are designed to tradeoff volume with efficiency to achieve miniaturized packaging. One major consequence of such design requirement is the building of excess heat within the thermal components and especially from the microprocessor of most electronic systems. Consequently, an inefficient removal of excess heat would build up around the electronic circuitry would lead to the eventual damage to the system. However, one key approach to achieve miniaturised yet efficient heat dissipating systems is to enhance the thermal performance of the device through an increase in the heat transfer between the device surface and its environment using fins. Fins are passive extended surface used to enhance heat dissipation from the thermal surface of electronic systems through natural convection, normally with air as the cooling medium for electronic cooling. Passive cooling using fin gained its popularity following the work of [3], and its subsequent practical application in thermal systems validate its viability as a heat dissipation approach.

Most modern high-processing, compact electronic systems are often accompanied by various thermal challenges. Research into reliable thermal management using extended surfaces for such electronic systems under different operating conditions and parameters have been intensely investigated in the literature [4-7]. In view of such research pursuit, the consideration of surface roughness has been established as a viable approach to improved thermal management [8, 9]. In addition, [10] presents a study on the effects of random rough surface on the thermal performance of microfin. [11] applied the power series to analyse the thermal performance of rough micro-fins of three different profiles, namely, hyperbolic, trapezoidal and concave. The analysis of [10, 11] only considers the thermal performance of conductive-convective fins, whilst basing their works on the assumption of constant thermal properties. Such an assumption is not valid when a large temperature difference exists between the fin base and its tip. Moreover, [12] used the method of least square, whilst [13] applied homotopy analysis method to study the effects of uniform magnetic field on the heat transfer characteristics of rectangular fin. [14] applied the spectral element method, whilst [15] applied the forward and inverse solution to study the dynamics of fin under a conductive-convective-radiative environment. [16, 17] applied Haar wavelet collocation to carry out parametric studies on the thermal performance, thermal stability and design analyses of a porous fin with

temperature-dependent thermal properties and internal heat generation.

Nevertheless, to the best of our knowledge, there is no established literature either experimental or theoretical that investigates the thermal behaviour of rough surface micro-fin with variable thermal conductivity operating under a convective-radiative heat transfer with practical application to microprocessors.

In this paper, our aim is to investigate the simultaneous effect of surface roughness, porosity and magnetic field on the performance of porous micro-fins under a convective-radiative heat transfer mechanism. The developed thermal models are solved numerically using Chebychev spectral collocation method (CSCM). We carried out parametric studies using the numerical solutions to establish the influences of porosity, surface roughness, and magnetic field on the micro-fin thermal behaviour.

The rest of the paper is organised as follows: In Section II, we formulate the fin problem. The modelling of the fin surface roughness is presented in Section III. In Section IV, we present the spectral collocation technique and applied it to the developed models. The fin efficiency is highlighted in Section V, whilst the fin optimisation is discussed in Section VI. Section VII provides the results of the parametric study using the present approach. Finally, conclusions of the present investigation are presented in Section VIII.

II. FORMULATION OF THE PROBLEM

Fig. 1 shows a heat sink of a microprocessor made up of a micro-fin with surface roughness and porosity. The fin is of dimensional length L with thickness t and is exposed on both faces and subjected to a convective-radiative environment at temperature Ta. Assume there is no thermal contact resistance exists at the fin base and the fin tip is of adiabatic. In addition, if the temperature of the fin is invariant with time for one-dimensional heat flow, the governing equations for the heat transfer in the fin [18] is given as:

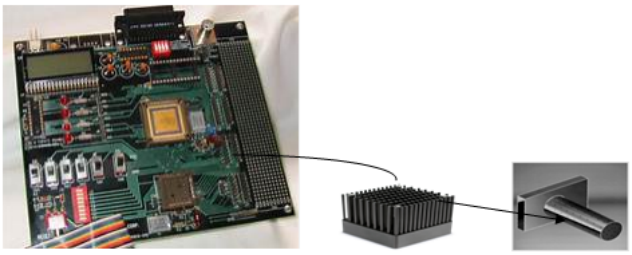

(a) (b) (c)

Fig. 1 (a) Motherboard of computer unit using heat sink (b) Picture representation of (b) heat sink with fin (c) cylindrical micro-fin

$$\frac{\partial}{\partial x}\left(k_{eff}(T)A_c\frac{\partial T}{\partial x}\right)-\frac{\rho wgK\beta c_p(T-T_a)^2}{\nu}-hp(T-T_a)-\sigma\varepsilon p\left(T^4-T_a^4\right)-\frac{J_c\times J_c}{\sigma}=0 \tag{1}$$

The boundary conditions are given as:

$$x=0,\ T=T_b$$

$$x=L,\ \frac{\partial T}{\partial x}=0 \tag{2}$$

The thermal conductivity of the micro-pin porous fins varies linearly [19] as:

$$k_{eff}(T)=\varphi k_f+(1-\varphi)k_s=k_{eff,a}A\left(1+\lambda\left(T-T_a\right)\right), \tag{3a}$$

and exponentially as

$$k_{eff}(T)=k_{a,eff}e^{\lambda(T-T_\infty)} \tag{3b}$$

Substituting Eqs. (3a) and (3b) into Eq. (1) becomes

$$k_{a,eff}\frac{\partial\overline{A_c}}{\partial x}\frac{\partial T}{\partial x}+k_{a,eff}\overline{A_c}\frac{\partial^2T}{\partial x^2}+k_{a,eff}\lambda(T-T_a)\frac{\partial\overline{A_c}}{\partial x}\frac{\partial T}{\partial x}+k_{a,eff}\lambda\overline{A_c}\left(\frac{\partial T}{\partial x}\right)^2+k_{a,eff}\lambda\overline{A_c}(T-T_a)\frac{\partial^2T}{\partial x^2}-\frac{\rho wgK\beta c_p(T-T_a)^2}{\nu}-hp(T-T_a)-\sigma\varepsilon p\left(T^4-T^4\right)-\frac{J_c\times J_c}{\sigma}=0 \tag{4}$$

If the thermal conductivity varies exponentially according to the law $k(T)=k_{a,eff}e^{\lambda(T-T_\infty)}$, then we have

$$k_{a,eff}e^{\lambda(T-T_\infty)}\frac{d\overline{A_c}}{dx}\frac{dT}{dx}+k_{a,eff}\lambda\overline{A_c}e^{\lambda(T-T_\infty)}\left(\frac{dT}{dx}\right)^2+k_{a,eff}\overline{A_c}e^{\lambda(T-T_\infty)}\frac{d^2T}{dx^2}-\frac{\rho wgK\beta c_p(T-T_a)^2}{\nu}-hp(T-T_a)-\sigma\varepsilon p\left(T^4-T_a^4\right)-\frac{J_c\times J_c}{\sigma}=0 \tag{5}$$

III. MODELLING OF THE SURFACE ROUGHNESS

Assuming the rough micro-fins have a random surface roughness that obeys the Gaussian probability distribution both in angular and longitudinal directions as shown in Fig. 2 and 3. Such an assumption is in line with the established assumptions found in [10, 11], and from [11], it can be shown that:

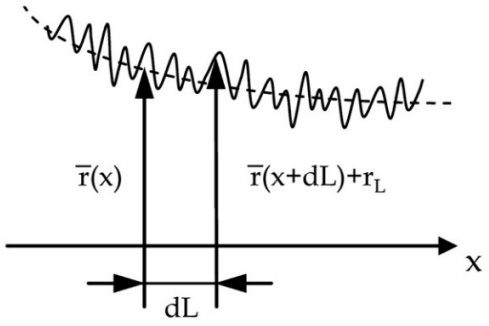

Fig. 2. Cross-sectional representation of generic pin fin with variable profile and rough surface

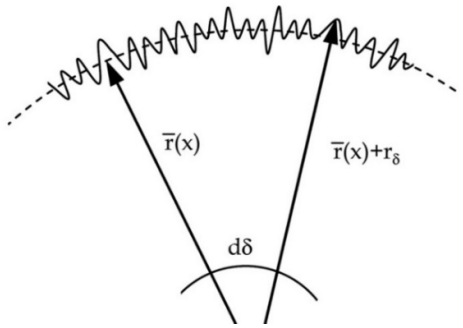

Fig. 3. Longitudinal-section of generic pin fin of variable profile and rough surface

$$\frac{\bar{A}_c(x)}{A_c(x)} = 1 + 2\left(\frac{\sigma}{\bar{r}(x)}\right)^2 \tag{6}$$

$$\frac{d\bar{A}_c}{dx} \approx \frac{dA_c}{dx} + 2\pi\bar{r}\left(x\right)m_\sigma = 2\pi\bar{r}\left(x\right)\sqrt{1+m_\sigma^2} \tag{7}$$

$$\bar{P}(x) = \frac{d\bar{A}_c}{dx} \approx 2\pi\bar{r}\left(x\right)\sqrt{1+m_\sigma^2} \tag{8}$$

where for a smooth perimeter, $P(x) = 2\pi\bar{r}\left(x\right)$

$$P(x) = P\left(x\right)\sqrt{1+m_\sigma^2} \tag{9}$$

and the mean for the absolute surface slope for roughness component is given as,

$$m_\sigma = \frac{1}{L}\int_0^L \left|\frac{\partial\left(r-r_b\right)}{dx}\right| dx \tag{10}$$

Taking the relative roughness as $\mathcal{E}$, we can define the roughness ratio as:

$$\mathrm{E} = \frac{\sigma}{r_b} \tag{11}$$

On substituting Eq. (11) into Eq. (6), we have

$$\bar{A}_c\left(x\right) = \left(1 + 2\left(\frac{r_b}{\bar{r}\left(x\right)}\right)^2 \mathrm{E}^2\right) A_c\left(x\right) \tag{12}$$

Substituting Eq. (7), (8), (9) and (12) into Eq. (5), we arrived at an energy equation for rough micro-fin as:

$$\begin{aligned}
&\frac{dA_c}{dx}\frac{dT}{dx} + 2\pi\bar{r}m_\sigma\frac{dT}{dx} + A_c\frac{d^2T}{dx^2} + 2\varepsilon^2 A_c\left(\frac{r_b}{\bar{r}}\right)^2\frac{d^2T}{dx^2} + \lambda\left(T-T_\infty\right)\frac{dA_c}{dx}\frac{dT}{dx} \\
&+2\pi\bar{r}m_\sigma\lambda\left(T-T_\infty\right)\frac{dT}{dx} + \lambda A_c\left(\frac{dT}{dx}\right)^2 + 2\varepsilon^2 A_c\lambda\left(\frac{r_b}{\bar{r}}\right)^2\left(\frac{dT}{dx}\right)^2 + \\
&A_c\lambda\left(T-T_\infty\right)\frac{d^2T}{dx^2} + 2\varepsilon^2 A_c\lambda\left(\frac{r_b}{\bar{r}}\right)^2\left(T-T_\infty\right)\frac{d^2T}{dx^2} \\
&-\frac{\rho wgK\beta c_p\sqrt{1+m_\sigma^2}\left(T-T_a\right)^2}{k_{a,eff}\nu} - \frac{h_b p\sqrt{1+m_\sigma^2}\left(T-T_a\right)}{k_{a,eff}} \\
&-\frac{\sigma\varepsilon p\sqrt{1+m_\sigma^2}\left(T^4-T_a^4\right)}{k_{a,eff}} - \frac{J_c\times J\sqrt{1+m_\sigma^2}_c}{\sigma k_{a,eff}} = 0
\end{aligned} \tag{13}$$

For cylindrical coordinate, A_c is constant, therefore $\frac{dA_c}{dx} = 0$

Where $\bar{r_c}(x) = r_b, P(\mathrm{x}) = 2\pi r_b \; and \quad A_c(\mathrm{x}) = \pi r_b^2$ (14)

Substituting Eq. (14) into Eq. (13), gives

$$\begin{aligned}
&\frac{d^2T}{dx^2} + \frac{2m_\sigma}{r_b}\frac{dT_c}{dx} + \frac{2\lambda m_\sigma}{r_b}\left(T_c-T_\infty\right)\frac{dT_c}{dx} + \lambda\left(\frac{dT_c}{dx}\right)^2 + 2\varepsilon^2\frac{d^2T_c}{dx^2} + \\
&2\varepsilon^2\lambda\left(\frac{dT_c}{dx}\right)^2 + \lambda\left(T_c-T_\infty\right)\frac{d^2T_c}{dx^2} + 2\varepsilon^2\lambda\frac{d^2T_c}{dx^2} \\
&-\frac{\rho wgK\beta c_p\sqrt{1+m_\sigma^2}\left(T-T_a\right)^2}{k_{a,eff}\nu} - \frac{h_b p\sqrt{1+m_\sigma^2}\left(T-T_a\right)}{k_{a,eff}} \\
&-\frac{\sigma\varepsilon p\sqrt{1+m_\sigma^2}\left(T^4-T_a^4\right)}{k_{a,eff}} - \frac{J_c\times J\sqrt{1+m_\sigma^2}}{\sigma k_{a,eff}} = 0
\end{aligned} \tag{15}$$

Also for the rough micro-fins with exponentially varying thermal conductivity, we have

$$\begin{aligned}
&\lambda A_c e^{\lambda(T-T_\infty)}\left(\frac{dT}{dx}\right)^2 + 2\lambda\varepsilon^2 A_c e^{\lambda(T-T_\infty)}\left(\frac{dT}{dx}\right)^2 + \frac{2m_\sigma}{r_b}e^{\lambda(T-T_\infty)}\frac{dT}{dx} + \\
&e^{\lambda(T-T_\infty)}\frac{\partial A_c}{\partial x}\frac{\partial T}{\partial x} + 2\pi\bar{r}m_\sigma e^{\lambda(T-T_\infty)}\frac{\partial T}{\partial x} + A_c e^{\lambda(T-T_\infty)}\left(\frac{\partial^2 T}{\partial x^2}\right) + \\
&2A_c\varepsilon^2\left(\frac{r_b}{r}\right)^2 e^{\lambda(T-T_\infty)}\left(\frac{\partial^2 T}{\partial x^2}\right) - \frac{\rho wgK\beta c_p\sqrt{1+m_\sigma^2}\left(T-T_a\right)^2}{k_{a,eff}\nu} - \\
&\frac{h_b p\sqrt{1+m_\sigma^2}\left(T-T_a\right)}{k_{a,eff}} - \frac{\sigma\varepsilon p\sqrt{1+m_\sigma^2}\left(T^4-T_a^4\right)}{k_{a,eff}} - \\
&\frac{J_c\times J\sqrt{1+m_\sigma^2}}{\sigma k_{a,eff}} = 0
\end{aligned} \tag{16}$$

For cylindrical coordinate, we arrived at

$$\begin{aligned}
&\lambda e^{\lambda(T_c-T_\infty)}\left(\frac{dT_c}{dx}\right)^2 + 2\lambda\varepsilon^2 e^{\lambda(T_c-T_\infty)}\left(\frac{dT_c}{dx}\right)^2 + \frac{2m_\sigma}{r_b}e^{\lambda(T_c-T_\infty)}\frac{dT_c}{dx} + \\
&e^{\lambda(T_c-T_\infty)}\frac{d^2T_c}{dx^2} + 2\varepsilon^2 e^{\lambda(T_c-T_\infty)}\frac{d^2T_c}{dx^2} - \frac{\rho wgK\beta c_p\sqrt{1+m_\sigma^2}\left(T-T_a\right)^2}{k_{a,eff}\nu} \\
&-\frac{h_b p\sqrt{1+m_\sigma^2}\left(T-T_a\right)}{k_{a,eff}} - \frac{\sigma\varepsilon p\sqrt{1+m_\sigma^2}\left(T^4-T_a^4\right)}{k_{a,eff}} - \frac{J_c\times J\sqrt{1+m_\sigma^2}_c}{\sigma k_{a,eff}} = 0
\end{aligned} \tag{17}$$

However, according to earlier work [37]

$$\frac{J_c\times J_c}{\sigma} = \sigma B_o^2 u^2 \tag{18}$$

Substituting Eq. (18) into Eq. (8), whilst taking the magnetic term as a linear function of temperature, we have $\bar{r_c}(x) = r_b$, $P(\mathrm{x}) = 2\pi r_b \; and \quad A_c(\mathrm{x}) = \pi r_b^2$. Substituting these into Eq. (17), gives

$$\frac{d^2T}{dx^2}+\frac{2m_\sigma}{r_b}\frac{dT_c}{dx}+\frac{2\lambda m_\sigma}{r_b}\left(T_c-T_\infty\right)\frac{dT_c}{dx}+\lambda\left(\frac{dT_c}{dx}\right)^2+2\varepsilon^2\frac{d^2T_c}{dx^2}+$$
$$2\varepsilon^2\lambda\left(\frac{dT_c}{dx}\right)^2+\lambda\left(T_c-T_\infty\right)\frac{d^2T_c}{dx^2}+2\varepsilon^2\lambda\frac{d^2T_c}{dx^2}$$
$$-\frac{\rho wgK\beta c_p\sqrt{1+m_\sigma^2}\left(T-T_a\right)^2}{k_{a,eff}\nu}-\frac{h_b p\sqrt{1+m_\sigma^2}\left(T-T_a\right)}{k_{a,eff}}$$
$$-\frac{\sigma\varepsilon p\sqrt{1+m_\sigma^2}\left(T^4-T_a^4\right)}{k_{a,eff}}-\frac{\sigma B_o^2u^2\sqrt{1+m_{\sigma_c}^2}}{k_{a,eff}}=0 \tag{19}$$

For cylindrical coordinate, we arrived at

$$\lambda e^{\lambda(T_c-T_\infty)}\left(\frac{dT_c}{dx}\right)^2+2\lambda\varepsilon^2e^{\lambda(T_c-T_\infty)}\left(\frac{dT_c}{dx}\right)^2+\frac{2m_\sigma}{r_b}e^{\lambda(T_c-T_\infty)}\frac{dT_c}{dx}+$$
$$e^{\lambda(T_c-T_\infty)}\frac{d^2T_c}{dx^2}+2\varepsilon^2e^{\lambda(T_c-T_\infty)}\frac{d^2T_c}{dx^2}-\frac{\rho wgK\beta c_p\sqrt{1+m_\sigma^2}\left(T-T_a\right)^2}{k_{a,eff}\nu}$$
$$-\frac{h_b p\sqrt{1+m_\sigma^2}\left(T-T_a\right)}{k_{a,eff}}-\frac{\sigma\varepsilon p\sqrt{1+m_\sigma^2}\left(T^4-T_a^4\right)}{k_{a,eff}}-\frac{\sigma B_o^2u^2\sqrt{1+m_{\sigma_c}^2}}{k_{a,eff}}=0 \tag{20}$$

Introducing the following dimensionless parameters of Eq. (21) into Eqs. (19) and (20),

$$\theta=\frac{T-T_a}{T-T_a},\quad \theta_a=\frac{T_a}{T_b-T_a},X=\frac{x}{L},\quad \lambda\left(T-T_\infty\right)=\beta_\lambda,\quad M_c^2=\frac{h_bL^2}{k_ar_b},$$
$$S_h=\frac{gk\beta L^2\left(T_b-T_a\right)^2}{\nu\alpha t};Nr=\frac{\varepsilon\sigma pL^2\left(T_b^3-T_a^3\right)}{k_aA};\quad \beta_c=\frac{x}{r_b}m_\sigma,\quad \alpha_c=\mathrm{E}^2 \tag{21}$$

we arrived at the dimensionless governing equations as for the rough micro-fin with linearly varying and exponentially varying thermal conductivity, respectively as:

$$\frac{d^2\theta}{dX^2}+\frac{2m_\sigma z_t}{r_b}\frac{d\theta}{dX}+\frac{2\beta_\lambda m_\sigma\theta z_t}{r_b}\frac{d\theta_c}{dX}+\beta_\lambda\left(\frac{d\theta}{dX}\right)^2+2\varepsilon^2\frac{d^2\theta}{dX^2}+$$
$$2\varepsilon^2\beta_\lambda\left(\frac{d\theta}{dX}\right)^2-\beta\theta_c\frac{d^2\theta}{dX^2}+2\varepsilon^2\lambda\frac{d^2\theta}{dX^2}-S_h\sqrt{1+m_\sigma^2}\theta^2$$
$$-2M_c^2\sqrt{1+m_\sigma^2}\theta-2Nr\sqrt{1+m_\sigma^2}\left[\left(\theta+\theta_a\right)^4-\theta_a^4\right]-Ha^2\sqrt{1+m_\sigma^2}\theta=0 \tag{22}$$

After expansion, we can

$$\frac{d^2\theta}{dX^2}+\frac{2m_\sigma z_t}{r_b}\frac{d\theta}{dX}+\frac{2\beta_\lambda m_\sigma\theta z_t}{r_b}\frac{d\theta_c}{dX}+\beta_\lambda\left(\frac{d\theta}{dX}\right)^2+2\varepsilon^2\frac{d^2\theta}{dX^2}+$$
$$2\varepsilon^2\beta_\lambda\left(\frac{d\theta}{dX}\right)^2-\beta\theta_c\frac{d^2\theta}{dX^2}+2\varepsilon^2\lambda\frac{d^2\theta}{dX^2}-S_h\sqrt{1+m_\sigma^2}\theta^2$$
$$-2M_c^2\sqrt{1+m_\sigma^2}\theta-2Nr\sqrt{1+m_\sigma^2}\theta^4-8Nr\sqrt{1+m_\sigma^2}\theta^3\theta_a$$
$$-12Nr\sqrt{1+m_\sigma^2}\theta^2\theta_a^2-8Nr\sqrt{1+m_\sigma^2}\theta\theta_a^3-Ha^2\sqrt{1+m_\sigma^2}\theta=0 \tag{23}$$

and

$$\beta_\lambda e^{\beta_\lambda\theta}\left(\frac{d\theta}{dX}\right)^2+2\beta_\lambda\alpha_c e\beta_\lambda^{\lambda\theta}\left(\frac{d\theta}{dX}\right)^2+2\gamma_c e^{\beta_\lambda\theta}\frac{d\theta}{dX}+$$
$$e\beta_\lambda^{\lambda\theta}\frac{d^2\theta}{dX^2}+2\alpha_c e^{\beta_\lambda\theta}\frac{d^2\theta}{dX^2}-S_h\sqrt{1+m_\sigma^2}\theta^2$$
$$-2M_c^2\sqrt{1+m_\sigma^2}\theta-2Nr\sqrt{1+m_\sigma^2}\theta^4-8Nr\sqrt{1+m_\sigma^2}\theta^3\theta_a$$
$$-12Nr\sqrt{1+m_\sigma^2}\theta^2\theta_a^2-8Nr\sqrt{1+m_\sigma^2}\theta\theta_a^3-Ha^2\sqrt{1+m_\sigma^2}\theta=0 \tag{24}$$

And the dimensionless boundary conditions are:

$$X=0,\quad \frac{d\theta}{dX}=0$$
$$X=1,\quad \theta=1.$$

(a) If the fin is smooth and the thermal conductivity varies linearly, we have:

$$\frac{d^2\theta_c}{d\psi^2}+\beta\theta\frac{d^2\theta_c}{d\psi^2}+\beta\left(\frac{d\theta_c}{d\psi}\right)^2-S_h\sqrt{1+m_\sigma^2}\theta^2$$
$$-2M_c^2\sqrt{1+m_\sigma^2}\theta-2Nr\sqrt{1+m_\sigma^2}\theta^4-8Nr\sqrt{1+m_\sigma^2}\theta^3\theta_a$$
$$-12Nr\sqrt{1+m_\sigma^2}\theta^2\theta_a^2-8Nr\sqrt{1+m_\sigma^2}\theta\theta_a^3-Ha^2\sqrt{1+m_\sigma^2}\theta=0 \tag{25}$$

(b) For the smooth fin with exponentially varying thermal conductivity

$$e^{\beta\theta_c}\frac{d^2\theta_c}{d\psi^2}+\beta e^{\beta\theta_c}\left(\frac{d\theta_c}{d\psi}\right)^2-S_h\sqrt{1+m_\sigma^2}\theta^2$$
$$-2M_c^2\sqrt{1+m_\sigma^2}\theta-2Nr\sqrt{1+m_\sigma^2}\theta^4-8Nr\sqrt{1+m_\sigma^2}\theta^3\theta_a$$
$$-12Nr\sqrt{1+m_\sigma^2}\theta^2\theta_a^2-8Nr\sqrt{1+m_\sigma^2}\theta\theta_a^3-Ha^2\sqrt{1+m_\sigma^2}\theta=0 \tag{26}$$

The dimensionless boundary conditions are given as

$$X=0,\quad \theta=1$$
$$X=1,\quad \frac{d\theta}{dX}=0 \tag{27}$$

In this work, the geometric ratio is given as $\xi=\frac{r}{L}$

IV. APPLICATION OF CHEBYSHEV COLLOCATION SPECTRAL METHOD

The development of exact analytical solutions for Eqs. (22) – (26) are very difficult if not an undaunting task to solve analytically. This is due to the nonlinearity of these equations. Therefore, as a means of taking recourse to numerical methods, we applied the Chebychev spectral collocation method (CSCM) in this work. The basic definition of the method and the detail procedures its applications can be found our previous publications [20]. Making a suitable transformation to map the physical domain [0, 1] into a computational domain [-1,1], we have:

$$\frac{\partial^2\widetilde{\theta}}{\partial x^2}+\frac{2m_\sigma z_t}{r_b}\frac{\partial\widetilde{\theta}}{\partial x}+\frac{2\beta_\lambda m_\sigma\widetilde{\theta}z_t}{r_b}\frac{\partial\widetilde{\theta}}{\partial x}+\beta_\lambda\left(\frac{\partial\widetilde{\theta}}{\partial x}\right)^2+2\varepsilon^2\frac{\partial^2\widetilde{\theta}}{\partial x^2}+$$
$$2\varepsilon^2\beta_\lambda\left(\frac{\partial\widetilde{\theta}}{\partial x}\right)^2-\beta\widetilde{\theta}_c\frac{\partial^2\widetilde{\theta}}{\partial x^2}+2\varepsilon^2\lambda\frac{\partial^2\widetilde{\theta}}{\partial x^2}-S_h\sqrt{1+m_c\theta^2}-2M_c^2\sqrt{1+m_c\widetilde{\theta}}-$$
$$2Nr\sqrt{1+m_\sigma^2\widetilde{\theta}^4}-8Nr\sqrt{1+m_\sigma^2\widetilde{\theta}^3\theta_a}-12Nr\sqrt{1+m_\sigma^2\widetilde{\theta}^2\theta_a^2}-$$
$$8Nr\sqrt{1+m_\sigma^2\widetilde{\theta}\theta_a^3}-Ha^2\sqrt{1+m_\sigma^2\widetilde{\theta}}=0 \tag{28}$$

and

$$\beta_\lambda e^{\beta_\lambda\widetilde{\theta}}\left(\frac{\partial\widetilde{\theta}}{\partial\psi}\right)^2+2\beta_\lambda\alpha_c e\beta_\lambda^{\lambda\widetilde{\theta}}\left(\frac{\partial\widetilde{\theta}}{\partial\psi}\right)^2+2\gamma_c e^{\beta_\lambda\widetilde{\theta}}\frac{\partial\widetilde{\theta}}{\partial\psi}+e\beta_\lambda^{\lambda\widetilde{\theta}}\frac{\partial^2\widetilde{\theta}}{\partial\psi^2}+$$
$$2\alpha_c e^{\beta_\lambda\widetilde{\theta}}\frac{\partial^2\widetilde{\theta}}{\partial\psi^2}-S_h\sqrt{1+m_\sigma^2\theta^2}-2M_c^2\sqrt{1+m_\sigma^2\widetilde{\theta}}-2Nr\sqrt{1+m_\sigma^2\widetilde{\theta}^4}-$$
$$8Nr\sqrt{1+m_\sigma^2\widetilde{\theta}^3\theta_a}-12Nr\sqrt{1+m_\sigma^2\widetilde{\theta}^2\theta_a^2}-8Nr\sqrt{1+m_\sigma^2\widetilde{\theta}\theta_a^3}-$$
$$Ha^2\sqrt{1+m_\sigma^2\widetilde{\theta}}=0 \tag{29}$$

In the same way, the transformation for the smooth micro-fin was done. Here, the boundary conditions are

$$\widetilde{\theta}(-1)=1,\quad \widetilde{\theta}'(1)=0 \tag{30}$$

$$\sum_{j=0}^{N}\partial_{jk}^2\widetilde{\theta}_c(X_j)+\frac{2m_\sigma z_t}{r_b}\sum_{j=0}^{N}\partial_{jk}^1\widetilde{\theta}(x_j)+\frac{2\beta_\lambda m_\sigma z_t}{r_b}\sum_{j=0}^{N}\widetilde{\theta}(x_j)\partial_{jk}^2\widetilde{\theta}(X_j)+$$
$$\beta_\lambda\left(\sum_{j=0}^{N}\partial_{jk}^1\widetilde{\theta}(x_j)\right)^2+2\varepsilon^2\sum_{j=0}^{N}\partial_{jk}^2\widetilde{\theta}_c(X_j)+2\varepsilon^2\beta_\lambda\left(\sum_{j=0}^{N}\partial_{jk}^1\widetilde{\theta}(x_j)\right)^2-$$
$$\beta\sum_{j=0}^{N}\widetilde{\theta}_c(x_j)\partial_{jk}^2\widetilde{\theta}_c(X_j)+2\varepsilon^2\lambda\sum_{j=0}^{N}\partial_{jk}^2\widetilde{\theta}_c(X_j)-S_k\sqrt{1+m_c^2}\widetilde{\theta}^2(X_j)-$$
$$2M_c^2\sqrt{1+m_c^2}\widetilde{\theta}^2(X_j)-2Nr\sqrt{1+m_c^2}\widetilde{\theta}^4(X_j)-8Nr\sqrt{1+m_c^2}\widetilde{\theta}^3(X_j)\theta_a-$$
$$12Nr\sqrt{1+m_c^2}\widetilde{\theta}^2(X_j)\theta_a^2-8Nr\sqrt{1+m_c^2}\widetilde{\theta}(X_j)\theta_a^3-Ha^2\sqrt{1+m_c^2}\widetilde{\theta}(X_j)=0 \tag{31}$$

and

$$\beta_\lambda\sum_{j=0}^{N}e^{\beta_\lambda\widetilde{\theta}_c}\partial_{jk}^2\widetilde{\theta}_c(X_j)+$$
$$2\beta_\lambda\alpha_c e^{\beta_\lambda\widetilde{\theta}_c}\sum_{j=0}^{N}e^{\beta_\lambda\widetilde{\theta}_c}\partial_{jk}^1\widetilde{\theta}_c(X_j)\sum_{j=0}^{N}e^{\beta_\lambda\widetilde{\theta}_c}\partial_{jk}^1\widetilde{\theta}_c(X_j)+$$
$$2\gamma_c\sum_{j=0}^{N}e^{\beta_\lambda\widetilde{\theta}_c}\partial_{jk}^1\widetilde{\theta}_c(X_j)+\sum_{j=0}^{N}e^{\beta_\lambda\widetilde{\theta}_c}\partial_{jk}^2\widetilde{\theta}_c(X_j)+$$
$$2\alpha_c\sum_{j=0}^{N}e^{\beta_\lambda\widetilde{\theta}_c}\partial_{jk}^2\widetilde{\theta}_c(X_j)-S_k\sqrt{1+m_c^2}\widetilde{\theta}^2(X_j)-$$
$$2M_c^2\sqrt{1+m_c^2}\widetilde{\theta}(X_j)-2Nr\sqrt{1+m_c^2}\widetilde{\theta}^4(X_j)-$$
$$8Nr\sqrt{1+m_c^2}\widetilde{\theta}^3(X_j)\theta_a-12Nr\sqrt{1+m_c^2}\widetilde{\theta}^2(X_j)\theta_a^2-$$
$$8Nr\sqrt{1+m_c^2}\widetilde{\theta}(X_j)\theta_a^3-Ha^2\sqrt{1+m_c^2}\widetilde{\theta}(X_j)=0 \tag{32}$$

The boundary conditions are

$$\sum d_{kj}^1\widetilde{\theta}(x_j)-0,\quad \widetilde{\theta}(x_j)=1 \tag{33}$$

The above Eq. (30) and (31) give systems of algebraic equations which are solved using Newton's iterative method.

V. FIN EFFICIENCY

The enhanced thermal behaviour of the micro-fin with artificial surface could be established through the determination of the fin efficiency as this is considered as the key performance indicator in the analysis of fin thermal performance. Following the definitions from our previous publications [20], it could be deduced that the efficiency of the fin is given as:

$$\eta=\frac{Q_f}{Q_{\max}}=\frac{\int_0^L\left\{\begin{array}{l}\frac{\rho wgK\beta c_p\sqrt{1+m_\sigma^2}(T-T_a)^2}{k_{a,eff}\nu}-\frac{h_b p\sqrt{1+m_\sigma^2}(T-T_a)}{k_{a,eff}}\\-\frac{\sigma\varepsilon p\sqrt{1+m_\sigma^2}(T^4-T_a^4)}{k_{a,eff}}-\frac{J_c\times J\sqrt{1+m_{\sigma_c}^2}}{\sigma k_{a,eff}}\end{array}\right\}dx}{\left\{\begin{array}{l}\frac{\rho wgK\beta c_p L\sqrt{1+m_\sigma^2}(T_b-T_a)^2}{k_{a,eff}\nu}-\frac{h_b pL\sqrt{1+m_\sigma^2}(T_b-T_a)}{k_{a,eff}}\\-\frac{\sigma\varepsilon pL\sqrt{1+m_\sigma^2}(T_b^4-T_a^4)}{k_{a,eff}}-\frac{J_c\times J\sqrt{1+m_{\sigma_c}^2}L}{\sigma k_{a,eff}}\end{array}\right\}} \tag{34}$$

Applying the dimensionless parameters, it can be shown that the dimensionless form of the efficiency is given as

$$\eta=\frac{Q_f}{Q_{\max}}=\frac{\int_0^L\left\{\begin{array}{l}S_h\sqrt{1+m_\sigma^2}\theta^2-2M_c^2\sqrt{1+m_\sigma^2}\theta\\-2Nr\sqrt{1+m_\sigma^2}\left[(\theta+\theta_a)^4-\theta_a^4\right]-Ha^2\sqrt{1+m_\sigma^2}\theta\end{array}\right\}dX}{\left\{\begin{array}{l}S_h\sqrt{1+m_\sigma^2}-2M_c^2\sqrt{1+m_\sigma^2}\\-2Nr\sqrt{1+m_\sigma^2}\left[(1+\theta_a)^4-\theta_a^4\right]-Ha^2\sqrt{1+m_\sigma^2}\end{array}\right\}} \tag{35}$$

Thus, the ratio of the efficiency of the rough fin to the smooth fin can be stated as:

$$\eta=\frac{\eta_{rough\_surface}}{\eta_{smooth\_surface}} \tag{36}$$

VI. FIN OPTIMIZATION

It is established that fin optimization could be achieved either by minimizing the volume (weight) for any required heat dissipation or maximizing the heat dissipation for any given fin volume [21-28]. In the present analysis, adopted the approach of maximizing the heat dissipation for any given fin volume.

By definition, the constant fin volume is defined as $V=A_c b$. therefore, the heat dissipation per unit volume is developed as

$$\frac{q_f}{V} = \frac{\int_0^L \left\{ \begin{array}{l} \dfrac{\rho w g K \beta c_p \sqrt{1+m_\sigma^{\,2}}\,(T-T_a)^2}{k_{a,eff}\nu} - \dfrac{h_b p \sqrt{1+m_\sigma^{\,2}}\,(T-T_a)}{k_{a,eff}} \\ - \dfrac{\sigma\varepsilon p \sqrt{1+m_\sigma^{\,2}}\,(T^4-T_a^4)}{k_{a,eff}} - \dfrac{J_c \times J\sqrt{1+m_{\sigma_c}^{\,2}}}{\sigma k_{a,eff}} \end{array} \right\} dx}{A_c b} \quad (37)$$

Eq. (37) can be written as

$$Q_f = \frac{q_f}{k(T_b - T_\infty)}\left(\frac{A_p}{V}\right) = \frac{A_p}{k(T_b - T_\infty)} \frac{\int_0^L \left\{ \begin{array}{l} \dfrac{\rho w g K \beta c_p \sqrt{1+m_\sigma^{\,2}}\,(T-T_a)^2}{k_{a,eff}\nu} - \dfrac{h_b p \sqrt{1+m_\sigma^{\,2}}\,(T-T_a)}{k_{a,eff}} \\ - \dfrac{\sigma\varepsilon p \sqrt{1+m_\sigma^{\,2}}\,(T^4-T_a^4)}{k_{a,eff}} - \dfrac{J_c \times J\sqrt{1+m_{\sigma_c}^{\,2}}}{\sigma k_{a,eff}} \end{array} \right\} dx}{A_c b} \quad (38)$$

where

$$A_p = \delta b$$

On substituting the dimensionless quantity in Eq. (21), we arrive at dimensionless form of the Eq. (38) is

$$Q_f = \frac{A_p L}{A_c b}\int_0^1 \left\{ \begin{array}{l} S_h \sqrt{1+m_\sigma^{\,2}}\,\theta^2 - 2M_c^{\,2}\sqrt{1+m_\sigma^{\,2}}\,\theta \\ -2Nr\sqrt{1+m_\sigma^{\,2}}\left[(\theta+\theta_a)^4 - \theta_a^4\right] - Ha^2\sqrt{1+m_\sigma^{\,2}}\,\theta \end{array} \right\} dX \quad (39)$$

VII. DISCUSSION

Fig. 4 – 13 show the graphical representation of the parametric study. The effects of geometrical ratio and nonlinear thermal conductivity variable on the temperature distribution, and consequently on the heat dissipation capacity of the rough micro-fin are shown in Fig. 4a and 4b. Although, increase in the nonlinear thermal conductivity parameter causes an increase in the temperature distribution. It could be seen from the figures that as the geometrical ratio increases, the temperature of the micro-fin drops further which depicts enhanced thermal performance in the fin.

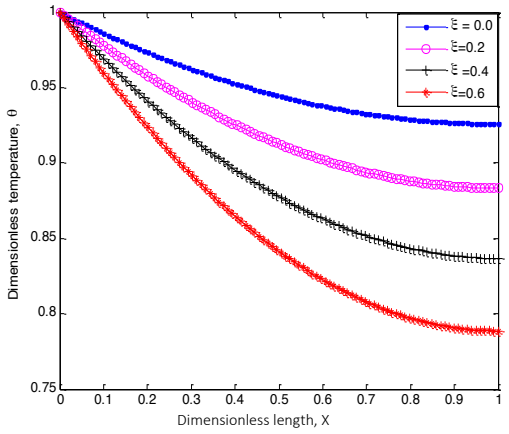

Fig. 4a. Effects of geometric ratio on fin temperature when β= 0.

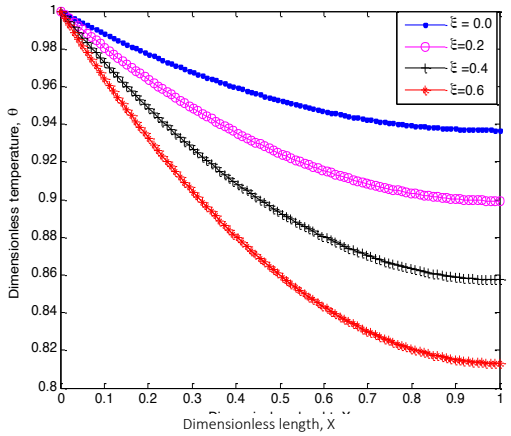

Fig. 4b. Effects of geometric ratio on fin temperature when $\beta = 1.0$

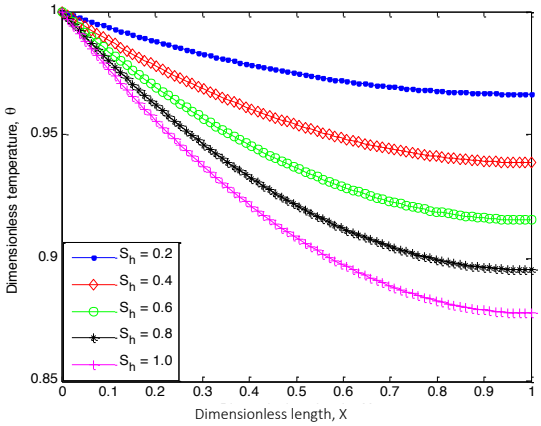

Fig. 5a. Effects of porosity on fin temperature when M= 0.5

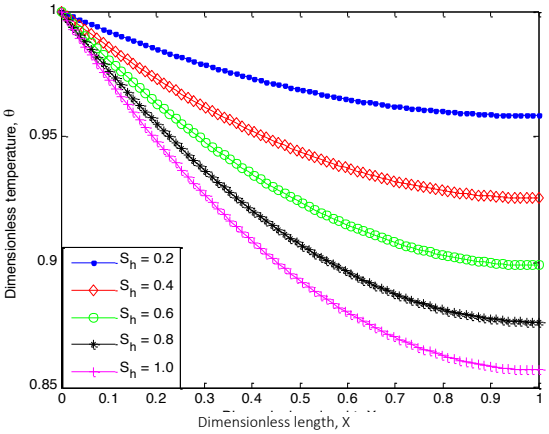

Fig. 5b. Effects of porosity on fin temperature when M = 1.0

The effects of porosity on the temperature of the fin are shown in Fig. 5a and 5b. As indicated in Fig. 5a and 5b, the fin temperature decreases rapidly as the porous parameters increases. This is because as the permeability of the porous fin increases, the porous parameter increases. Moreover, as permeability variable increases, the ability of the surrounding or cooling fluid around the fin increases to penetrate more through the fin pores, thereby increasing the buoyancy effect, which consequently increases the heat transferred through the fin.

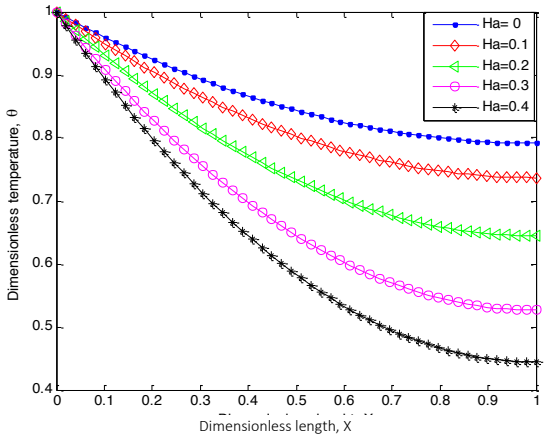

Fig. 6a. Effects of magnetic field parameter on fin temperature when M= 0.5

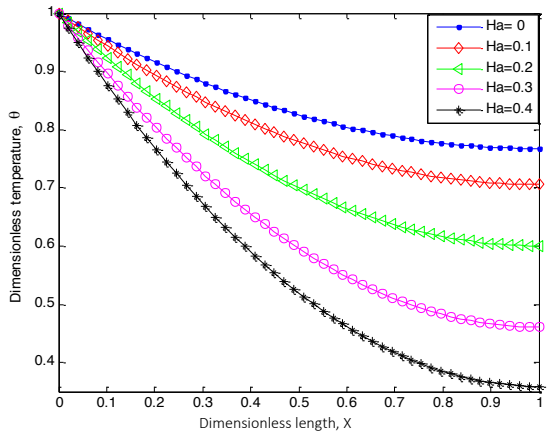

Fig. 6b. Effects of magnetic field parameter on fin temperature when M = 1.0

Fig. 6a and 6b highlight the effects of the magnetic field parameter i.e. the Hartmann number on the performance of the micro-fin. From Fig. 6a and 6b, increase in the Hartman number enhance the performance of the fin. The improved thermal behaviour of the fin is due to the fact that, as the magnetic field parameter increases, it causes the magnetic force to increase, which invariably increases the magnetic field strength and the convective heat transfer mechanism. The presence of the magnetic field affects the buoyancy force to increase by increasing the coefficient of heat transfer, making the fin to transfer more heat by the convective and radiative mechanism. The direction of the magnetic field is transverse. It affects the convection near the fins by increasing the rate of convective heat transfer. Convective heat transfer coefficient increases locally in the region where magnetic field exists. The convective heat transfer coefficient is directly proportional to the velocity of the fluid surrounding the fin. The transverse magnetic field increases the velocity of the fluid surrounding the fin which consequently increases the convective heat transfer coefficient. Therefore, through the enhanced convective heat transfer coefficient, the magnetic field increases the convection by increases the velocity of the fluid surrounding the fin. then the rate of convective heat transfer is increased. This in effect results in enhanced heat transfer from the fin and consequently improve the thermal performance of the fin. Thus, from the parametric analysis, we established that increase in the magnetic field, improves the fin efficiency due to increase in convective heat transfer. This finding agrees with the works of [12, 29].

The influence of convective heat transfer and magnetic field can be recorded either at a low or high temperature process. However, the radiative heat transfer will be dominant when there is relatively high temperature difference between the fin and its surroundings. Although, the percentage contribution of magnetic field, convective and radiative heat transfer in the heat transfer process are not fixed values for all the cases considered, in this work, we have used a scenario to show the contribution of the radiation component as depicted in Fig. 7.

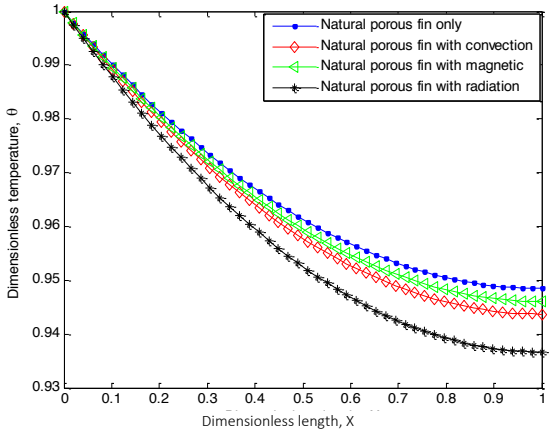

Fig. 7. Effects of convective, magnetic and radiative parameter on fin temperature

Fig. 8a and 8b shows the effect of the radiative parameter on the fin thermal behaviour. From the figures, it is established that the presence of radiative heat transfer increases the performance of the fin. In addition, the effects of thermal conductivity of the rough micro-fins on temperature distribution with varying thermo-geometric parameter of 0.5 and 1.0 are shown in Fig. 9a and 9b.

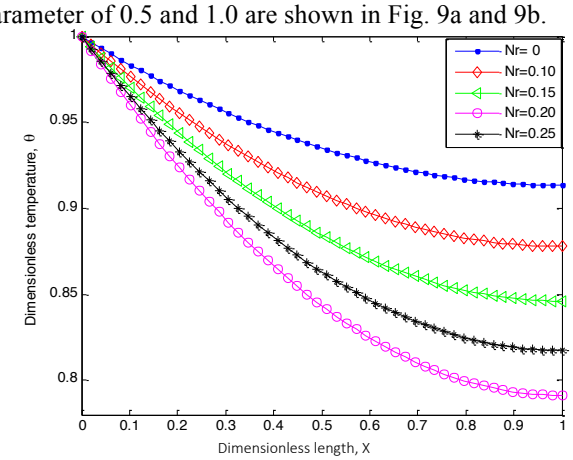

Fig. 8a. Effects of the radiative parameter on fin temperature when *M*= 0.5

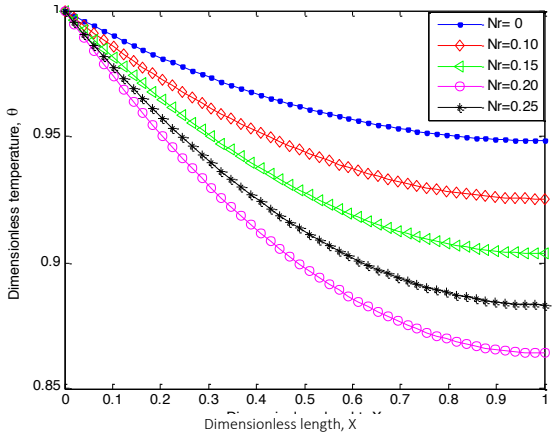

Fig. 8b. Effects of radiative parameter on fin temperature when M = 1.0

From Fig. 9a and 9b, we show that the increased nonlinear thermal conductivity parameter reduces the rate of heat transfer in the micro-fin, i.e. as the temperature of the fin drops, the value of the nonlinear thermal conductivity parameter increases. This trend is recorded for the study of the effect of the thermo-geometric parameter on the thermal performance of the fin as shown in Fig 10 and 11. Furthermore, this result also represents the effects of increased thermal conductivity using different materials for determining the performance of the fin.

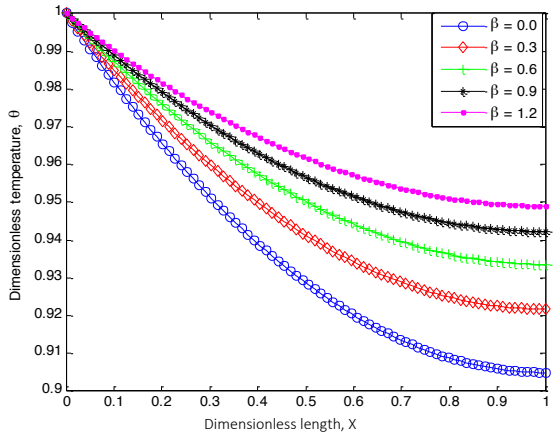

Fig. 9a Effects of β on fin temperature when M_c = 0.5

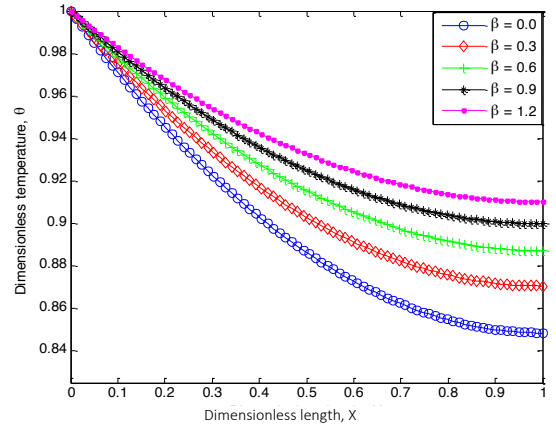

Fig. 9b Effects of β on fin temperature when M_c = 1.0

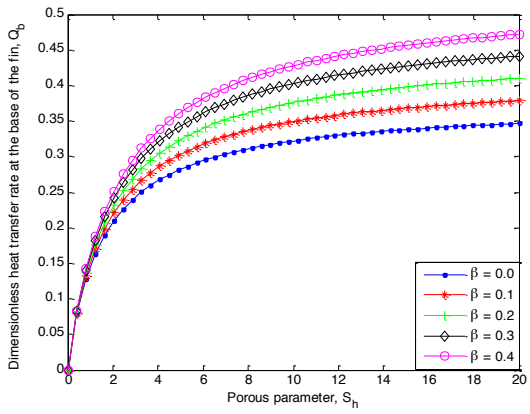

Fig. 10a. Effects of thermal conductivity parameter on fin temperature when M=0.5

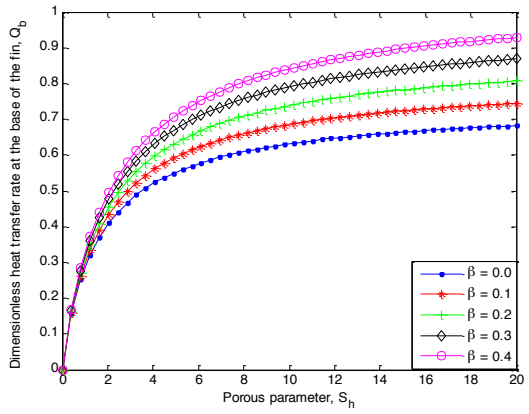

Fig. 10b. Effects of thermal conductivity parameter on fin temperature when M = 1.0

Using the heat dissipated through the fin as a performance indicator, it can be inferred from Figs. 9a-9b and 10a-10b that the thermal conductivity parameter significantly affects heat transferred at the base of the fin. Moreover, the rate of heat transfer increases as the thermal conductivity parameter increases.

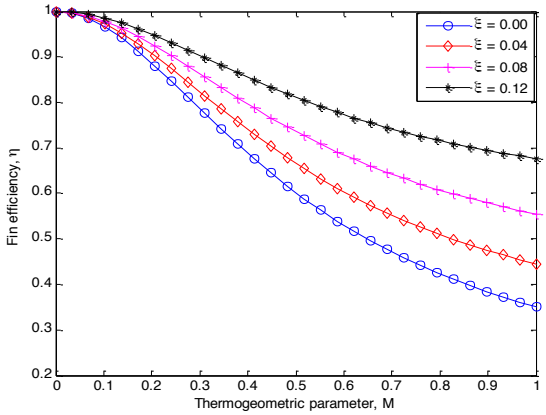

Fig. 11. Effects of geometrical ratio on fin efficiency

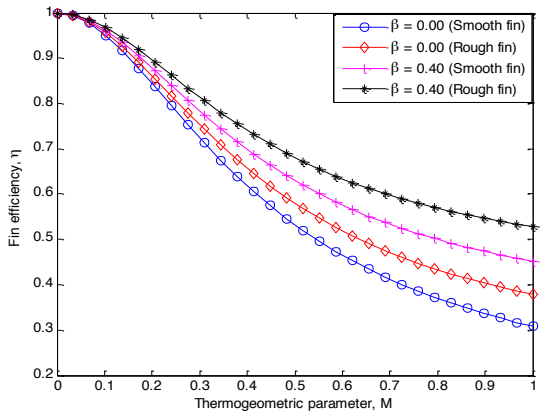

Fig. 12. Effects of thermal conductivity and surface roughness on the efficiency of the micro-fin

Fig. 11 and 12, shows that the geometric ratio, nonlinear thermal conductivity parameter and the surface roughness of the micro-fin significantly affects the thermal efficiency of the micro-fin. This establishes that the geometric ratio and surface roughness of the fin enhance the thermal performance of the fin. Moreover, the result shows that the artificial rough surface creates a thin or thick layer on the fin; depending on the thickness of the roughness, and the base of the rough fin. Nonetheless, this layer increases the thermal resistance of the solid-fluid interface with the heat flow resulting in a higher temperature at the surface of the fin.

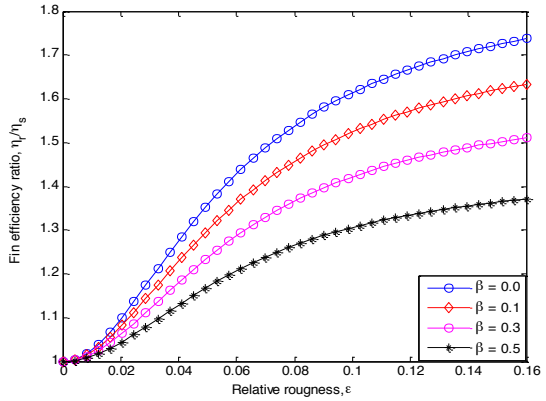

Fig. 13. Effects of thermal conductivity on fin efficiency ratio when M=0.5

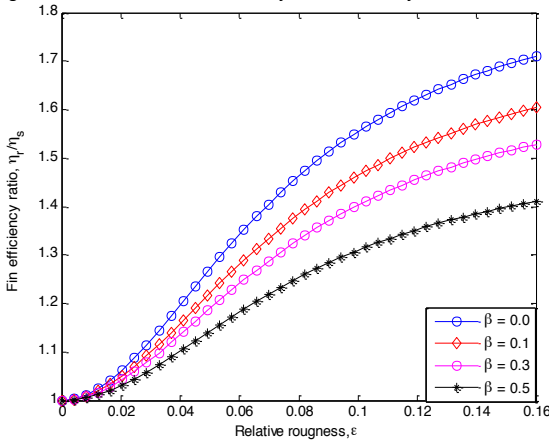

Fig. 14. Effects of thermal conductivity on fin efficiency ratio when M=1.0

Fig. 13 and Fig. 14 show the effects of thermal conductivity and artificial surface roughness on the fin efficiency ratio. Fin efficiency ratio which describes the ratio of the efficiency of the rough fin to the efficiency of the smooth fin is shown in Fig 13 and 14 to be greater than unity. This depicts an enhanced thermal performance in the rough fin as compared to the smooth fin. In addition, the fin surface roughness increases the thermal efficiency of the fin due to increase in temperature uniformity in the rough fin. This consequently causes an increase in the temperature difference between the rough micro-fin and the bulk temperature.

Based on the using the approach of maximizing the heat dissipation for any given fin volume, the variation of the non-dimensional heat transfers Q/ζ with thermo-geometric parameter M for different values the non-linear thermal conductivity terms, β, under a given profile area, A_p is given in Fig. 15. From the results in the figure, the heat transfer first rises and then falls as the fin length increases. It is established form the figure that the optimum fin length increases as β increases. Using Fig. 16, one can obtain the optimum dimensions of the fin for the different values of variable thermal conductivity.

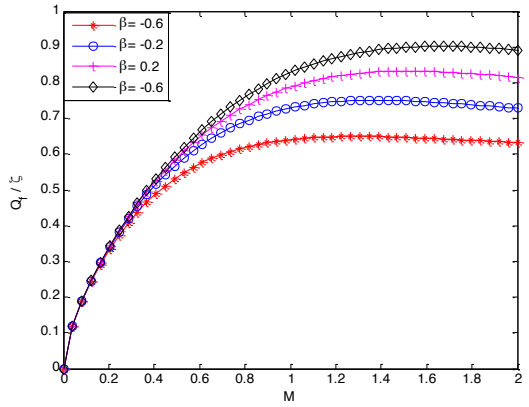

Fig. 15. Effects of non-linear thermal conductivity and thermo-geometric parameters on the dimensionless heat transfer, Q_f/ζ

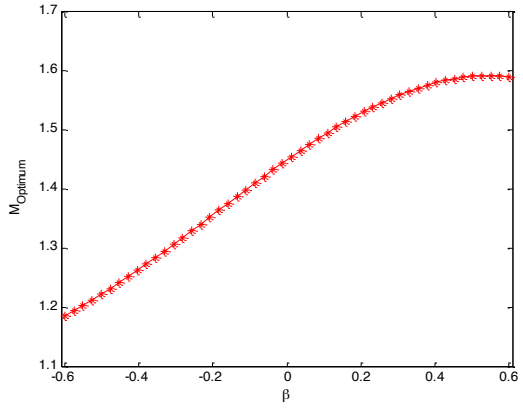

Fig. 16. Effects of non-linear thermal conductivity parameter on the optimum thermo-geometric parameter

The results of CSCM are verified using fourth-order Runge-Kutta coupled with shooting method and also, with the results of an approximate analytical technique (homotopy perturbation method) as addressed in the peer-reviewed literature. The comparison of results is shown in the Table 1 of the revised manuscript.

Table 1: Comparison of results *for θ(X) for S_h = 0.5, Nc = 0.3, Nr = 0.2, H = 0.1, ε = 0.0, m_σ=0.0, β_λ=0.0*

X	NM [39]	HPM [39]	CSCM
0.00	0.863499231	0.863499664	0.863499453
0.05	0.863828568	0.863829046	0.863828133
0.10	0.864817090	0.864817539	0.864817261
0.15	0.866466182	0.866465743	0.866466317
0.20	0.868776709	0.868776261	0.868776516
0.25	0.871751555	0.871751104	0.871751429
0.30	0.875393859	0.875393404	0.875393678
0.35	0.879707472	0.879707010	0.879707292
0.40	0.884696967	0.884696500	0.884696854
0.45	0.890367650	0.890367181	0.890367569
0.50	0.896725569	0.896725096	0.896725347
0.55	0.903777531	0.903777060	0.903777350
0.60	0.911531120	0.911530658	0.911531257
0.65	0.919994710	0.919994259	0.919994671
0.70	0.929177488	0.929177056	0.929177392
0.75	0.939089476	0.939089079	0.939089275
0.80	0.949741555	0.949741203	0.949741475
0.85	0.961145491	0.961145189	0.961145349
0.90	0.973313964	0.973313764	0.973313893
0.95	0.986260599	0.986260549	0.986260456
1.00	1.000000000	1.000000000	1.000000000

The results presented in the table establish the high accuracy of the CSCM as it agrees very well with the results numerical and approximate analytical method.

VIII. CONCLUSION

In this work, a numerical investigation of the simultaneous effects of artificial surface roughness, porosity and magnetic field on the performance of rough porous micro-fins of microprocessors in a convective-radiative environment is carried out using Chebychev spectral collocation method. The numerical solutions of the developed thermal models are used to conduct the parametric analysis, and to establish the thermal performance enhancement of the rough fins over the existing smooth fins. The results show the effects of pores in the fin, applied magnetic field, geometric ratio and the surface roughness in enhancing the thermal performance of the fin in a convective-radiative environment. However, the performance of the fin decreases when it operates only in a convective environment. Furthermore, the investigation established that the fin efficiency ratio is greater than unity for the rough surface fin when the rough and smooth fins are subjected to the same operational conditions using the same geometrical, physical, thermal and material properties. Therefore, improved thermal management of electronic and thermal systems can be achieved using a heat sink with artificial rough surface fins with porosity under the influence of a magnetic field.

NOMENCLATURE

A_b Fin base cross-sectional area, m^2
A_c Cross-sectional area of the fin, m^2
$\bar{A}_c$ Average cross-sectional area of the rough fin, m^2
A_s Surface area of the fin exposed to convection, m^2
$\bar{A}_s$ Average surface area of the rough fin exposed to Convection, m^2
B_i Biot number, given by $2r_b h/k$
$B0$ Magnetic field intensity, T
c_p Specific heat of the fluid through porous fin, *J/kg-K*
g Gravity constant, *m/s²*
h Heat transfer coefficient, W/m^2K
Jc Conduction current intensity, A
k fin thermal conductivity, $Wm^{-1}K^{-1}$
k_f fin thermal conductivity of fluid, $Wm^{-1}K^{-1}$
k_s fin thermal conductivity of solid, $Wm^{-1}K^{-1}$
k_{eff} effective thermal conductivity of fin, $Wm^{-1}K^{-1}$
Ha Hartmann number
Nr radiation parameter
S_h porosity parameter
X dimensionless length of the fin
K Permeability of the porous fin (m^2)
L Fin length, m^2
m Thermo-geometric parameter, m^{-1}
m_σ Mean absolute surface slope
M^2 Extended Biot number
n Heat transfer coefficient constant
P Fin perimeter, m
q Heat transfer rate, W
r Fin radius, m
$\bar{r}$ Average radius of a rough fin, m
r_δ Random variation of the fin radius in the angular direction, m
r_b Fin base radius, m
r_L Random variation of the fin radius in the longitudinal direction, m
r_t Fin tip radius, m
T Temperature, K
T_b Fin base temperature, K
x Longitudinal coordinate, m
x_b Location of the base for the hyperbolic fin, m
x_t Location of the tip for the hyperbolic fin, m
x Axial length measured from fin tip (m)
z Longitudinal coordinate, m

Greek symbols

ε relative roughness
φ dimensionless coordinate
η fin efficiency
λ length of the arc of the fin profile, m
θ dimensionless temperature
σ isotropic surface roughness, m
σ_δ fin surface roughness in angular direction, m
σ_L fin surface roughness in longitudinal direction, m
ξ geometric ratio
ψ dimensionless coordinate
ρ density of the fluid
ν Kinematic viscosity, $m^2 s^{-1}$
σ Electric conductivity, S/m
σ Stefan–Boltzmann constant, $Wm^2 K^4$
β thermal conductivity parameter
δ thickness of the fin, m
θ dimensionless temperature
β' coefficient of thermal expansion, K^{-1}
∅ porous fraction

Subscripts

s solid properties
f fluid properties
eff effective porous properties

ACKNOWLEDGMENT

This work is supported in part by the Tertiary Education Trust Fund (TETFund) of the Federal Republic of Nigeria.

REFERENCE

[1] G. E. Moore, "Cramming more components onto integrated circuits, Reprinted from Electronics, volume 38, number 8, April 19, 1965, pp.114 ff," *IEEE Solid-State Circuits Society Newsletter,* vol. 11, pp. 33-35, 2006.

[2] R. Mahajan, C. Chia-pin, and G. Chrysler, "Cooling a Microprocessor Chip," *Proceedings of the IEEE,* vol. 94, pp. 1476-1486, 2006.

[3] S. Kiwan and M. A. Al-Nimr, "Using Porous Fins for Heat Transfer Enhancement," *Journal of Heat Transfer,* vol. 123, pp. 790-795, 2000.

[4] S. V. Garimella, A. S. Fleischer, J. Y. Murthy, A. Keshavarzi, R. Prasher, C. Patel, *et al.*, "Thermal Challenges in Next-Generation Electronic Systems," *IEEE Transactions on Components and Packaging Technologies,* vol. 31, pp. 801-815, 2008.

[5] W. A. Khan, J. R. Culham, and M. M. Yovanovich, "The Role of Fin Geometry in Heat Sink Performance," *Journal of Electronic Packaging,* vol. 128, pp. 324-330, 2006.

[6] C. J. Shih and G. C. Liu, "Optimal design methodology of plate-fin heat sinks for electronic cooling using entropy generation strategy," *IEEE Transactions on Components and Packaging Technologies,* vol. 27, pp. 551-559, 2004.

[7] G. Oguntala and R. Abd-Alhameed, "Performance of convective-radiative porous fin heat sink under the influence of particle deposition and adhesion for thermal enhancement of electronic components," *Karbala International Journal of Modern Science,* 2018/07/07/ 2018.

[8] F. Zhou, G. W. DeMoulin, D. J. Geb, and I. Catton, "Closure for a plane fin heat sink with scale-roughened surfaces for volume averaging theory (VAT) based modeling," *International Journal of Heat and Mass Transfer,* vol. 55, pp. 7677-7685, 2012/12/01/ 2012.

[9] L. Ventola, F. Robotti, M. Dialameh, F. Calignano, D. Manfredi, E. Chiavazzo, *et al.*, "Rough surfaces with enhanced heat transfer for electronics cooling by direct metal laser sintering," *International Journal of Heat and Mass Transfer,* vol. 75, pp. 58-74, 2014/08/01/ 2014.

[10] M. Bahrami, M. M. Yovanovich, and R. J. Culham, "Role of Random Roughness on Thermal Performance of Microfins," *Journal of Thermophysics and Heat Transfer,* vol. 21, pp. 153-157, 2007/01/01 2007.

[11] L. I. Díez, S. Espatolero, C. Cortés, and A. Campo, "Thermal analysis of rough micro-fins of variable cross-section by the power series method," *International Journal of Thermal Sciences,* vol. 49, pp. 23-35, 2010/01/01/ 2010.

[12] H. Hoshyar, Ganji, DD, Majidian, AR, "Least Square Method for Porous Fin in the Presence of Uniform Magnetic Field " *Journal of Applied Fluid Mechanics,* vol. 9, pp. 661-668, 2016.

[13] S. G. Rezazadeh, D.D; Salaryan, h, "Determination of Temperature Distribution for Porous Fin Which Is Exposed to Uniform Magnetic Field to a Vertical Isothermal Surface by Homotopy Analysis Method and Collocation Method," *Indian Journal of Scientific Research,* vol. 1, pp. 215-222, 2014.

[14] J. S. Ma, Yasong; Li, Benwen, "Simulation of combined conductive, convective and radiative heat transfer in moving irregular porous fins by spectral element method," *International Journal of Thermal Sciences,* vol. 118, pp. 475-487, 2017/08/01/ 2017.

[15] R. Das, "Forward and inverse solutions of a conductive, convective and radiative cylindrical porous fin," *Energy Conversion and Management,* vol. 87, pp. 96-106, 2014/11/01/ 2014.

[16] G. A. Oguntala and R. A. Abd-Alhameed, "Haar Wavelet Collocation Method for Thermal Analysis of Porous Fin with Temperature-dependent Thermal Conductivity and Internal Heat Generation," *Journal of Applied and Computational Mechanics,* vol. 3, pp. 185-191, 2017.

[17] G. Oguntala, R. Abd-Alhameed, G. Sobamowo, and I. Danjuma, "Performance, Thermal Stability and Optimum Design Analyses of Rectangular Fin with Temperature-Dependent Thermal Properties and Internal Heat Generation," *Journal of Computational Applied Mechanics,* vol. 49, pp. 37-43, 2018.

[18] G. Oguntala, R. Abd-Alhameed, and G. Sobamowo, "On the effect of magnetic field on thermal performance of convective-radiative fin with temperature-dependent thermal conductivity," *Karbala International Journal of Modern Science,* vol. 4, pp. 1-11, 2018/03/01/ 2018.

[19] M. G. Sobamowo, O. M. Kamiyo, and O. A. Adeleye, "Thermal performance analysis of a natural convection porous fin with temperature-dependent thermal conductivity and internal heat generation," *Thermal Science and Engineering Progress,* vol. 1, pp. 39-52, 2017/03/01/ 2017.

[20] G. A. Oguntala, R. A. Abd-Alhameed, G. M. Sobamowo, and E. Nnabuike, "Effects of Particles Deposition on Thermal Performance of a Convective-Radiative Heat Sink Porous Fin of an Electronic Component," *Thermal Science and Engineering Progress,* 2017/10/28/ 2017.

[21] R. K. Irey, "Errors in the One-Dimensional Fin Solution," *Journal of Heat Transfer* vol. 90, pp. 175-176 1968.

[22] W. Lau and W. Tan, "Errors in One-Dimensional Heat Transfer Analysis in Straight and Annular Fins," *Journal of Heat Transfer,* vol. 95, 01/11/1973 1973.

[23] P. Razelos and K. Imre, "The Optimum Dimensions of Circular Fins with Variable Thermal Parameters," *Journal of Heat Transfer,* vol. 102, pp. 420-425, 1980.

[24] P. Razelos and K. Imre, "Minimum mass convective fins with variable heat transfer coefficients," *Journal of the Franklin Institute,* vol. 315, pp. 269-282, 1983/04/01/ 1983.

[25] H. C. Unal, "Determination of the temperature distribution in an extended surface with a non-uniform heat Effect of the boundary condition at a fin tip on the performance of the fin 1495 transfer coefficient,," *Int. J. Heat Mass Transfer* vol. 28, pp. 2279-2284, 1985.

[26] A. N. Hrymak, G. J. McRae, and A. W. Westerberg, "Combined Analysis and Optimization of Extended Heat Transfer Surfaces," *Journal of Heat Transfer,* vol. 107, pp. 527-532, 1985.

[27] K. Laor and H. Kalman, "The effect of tip convection on the performance and optimum dimensions of cooling fins," *International Communications in Heat and Mass Transfer,* vol. 19, pp. 569-584, 1992/07/01/ 1992.

[28] T. Mutlu and T. Al-Shemmeri, "Steady-state and transient performance of a shrouded Longitudinal fin array," *International Communication of Heat and Mass Transfer* vol. 20, pp. 133–143, 1993.

[29] S. Rezazadeh Amirkolaei, Ganji, DD, Salarian, H, "Determination Of Temperature Distribution For Porous Fin Which Is Exposed To Uniform Magnetic Field To A Vertical Isothermal Surface By Homotopy Analysis Method And Collocation Method," *Indian Journal of Scientific Research,* vol. 1, pp. 215-222, 2014.

George A. Oguntala (*M'13*) received the B.S. degree in Electronics/Computer Engineering, M.S in Engineering Analysis. He is currently pursuing the Ph.D. degree in Electrical Engineering at the University of Bradford, UK.

Mr. Oguntala is a Chartered engineer, and a member of the Institution of Engineering and Technology, UK, Nigerian Institution of Electrical Electronics Engineers, Nigeria Society of Engineers and the Engineering Council. His research interest includes applied and computational mathematics, energy systems, antenna and propagation, RFID, digital Healthcare and IoT.

Gbeminiyi M. Sobamowo received the B.S., M.S. and Ph.D. degree all in mechanical engineering from University of Lagos, Akoka, Lagos, Nigeria, in 2013.

He is a Lecturer with the Mechanical Engineering Department, University of Lagos. His research interests include energy systems modelling, simulation and design, renewable energy systems, flow and heat transfer and thermal fluidic induced instability in energy systems. He is a member of the Nigerian Institution of Mechanical Engineers, Nigeria Society of Engineers, and the Engineering Council.

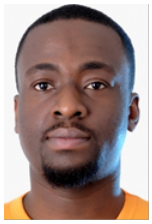

Nnabuike N. Eya (*M'16*) received the B.S. degree and M.S. in Computer Science from Teesside University, Middlesbrough, UK. He is currently pursuing his PhD degree in Electrical Engineering and Computer Science at the University of Bradford, UK.

His research interests include: computational analysis, multi-user multi-service security, mobility management, network security, cryptography and information privacy.

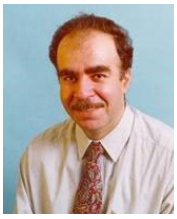

Raed Abd-Alhameed (M'02, S'13) is Professor of Electromagnetic and Radio Frequency Engineering at the University of Bradford, UK. He has long years' research experience in the areas of Radio Frequency, Signal Processing, propagations, antennas and electromagnetic computational techniques, and has published over 500 academic journal and conference papers; in addition he is co-authors of four books and several book chapters. At the present he is the leader of Radio Frequency, Propagation, sensor design and Signal Processing; in addition to leading the Communications research group for years within the School of Engineering and Informatics, Bradford University, UK. He is Principal Investigator for several funded applications to EPSRCs and leader of several successful knowledge Transfer Programmes such as with Arris (previously known as Pace plc), Yorkshire Water plc, Harvard Engineering plc, IETG ltd, Seven Technologies Group, Emkay ltd, and Two World Ltd. He has also been a co-investigator in several funded research projects including: 1) H2020 MARIE Skłodowska-CURIE ACTIONS: Innovative Training Networks (ITN) "Secure Network Coding for Next Generation Mobile Small Cells 5G-US", 2) Nonlinear and demodulation mechanisms in biological tissue (Dept. of Health, Mobile Telecommunications & Health Research Programme and 3) Assessment of the Potential Direct Effects of Cellular Phones on the Nervous System (EU: collaboration with 6 other major research organizations across Europe). He was awarded the business Innovation Award for his successful KTP with Pace and Datong companies on the design and implementation of MIMO sensor systems and antenna array design for service localizations. He is the chair of several successful workshops on Energy Efficient and Reconfigurable Transceivers (EERT): Approach towards Energy Conservation and CO2 Reduction that addresses the biggest challenges for the future wireless systems. He has also appointed as a guest editor for the IET Science, Measurements and Technology Journal since 2009, and 2012. He is also a research visitor for Wrexham University, Wales since Sept 2009 covering the wireless and communications research areas. Professor Abd-Alhameed has also been elected as UK panel member, for International Union of Radio Science (URSI), Commission K from 2018. His interest in computational methods and optimizations, wireless and Mobile communications, sensor design, EMC, beam steering antennas, Energy efficient PAs, RF predistorter design applications. He is the Fellow of the Institution of Engineering and Technology, Fellow of Higher Education Academy and a Chartered Engineer.